A Wireless System For Real-Time Environmental And Energy Monitoring Of A Metro Station: Lessons Learnt From A Three-Year Research Project

Maddalena Nurchis[a], Mikko Valta[a], Massimo Vaccarini[b], Alessandro Carbonari[b]

[a] VTT Technical Research Centre of Finland - Kaitoväylä 1, 90571 Oulu, Finland
[b] Università Politecnica delle Marche, Department of Civil and Building Engineering and Architecture (DICEA), via Brecce Bianche, 60131, Ancona, Italy
E-mail: maddalena.nurchis@gmail.com , Mikko.Valta@vtt.fi , m.vaccarini@univpm.it , alessandro.carbonari@univpm.it

ABSTRACT

Optimal energy management of underground transportation systems is widely recognized as a key aspect for significant energy savings at regional level. The three-year long EU funded "Seam4us" research project (2011 to 2014) aims to create a system for optimized integrated energy management, relying on the Passeig de Gracia metro station in Barcelona as the pilot station. One of the outcomes of the project was the installation of a wireless sensor network, in order to track in real time both environmental and energy parameters. The data collected by the network have been exploited to inform an intelligent control system about the state of the station. In fact, a reliable real-time sensing is critical for implementing advanced control policies in any kind of environment. For that reason, this paper will report on the Seam4us findings regarding real-time sensing of that quite harsh domain. The design criteria and constraints that led to the final installation will be argued. Then, post-processing functions, i.e. those algorithms turning raw data into the variables which can be processed by the controller, will be described. Finally, the general performance of the system will be discussed, in terms of reliability of data exchange and energy efficiency.

Keywords –
Real-time monitoring; environmental tracking; building control systems

1 Introduction

In this paper the suitability of cost-effective technologies for real-time measurement of environmental parameters in the "Passeig de Gracia" (PdG) subway station (Line no. 3) in Barcelona are reported. This monitoring platform is in charge of gathering data from sensors, re-arranging and post-processing them into a database, and forwarding clean, time aligned measurements to the intelligent control unit, that is in charge of applying optimum control policies for energy savings. The whole control system was the objective of the EU project SEAM4US (Sustainable Energy mAnageMent for Underground Stations) [1], which aims at optimizing the operation of mechanical air supply, lighting and passenger movements. In this paper, we will focus on the Wireless Sensor Network (WSN) and on the post-processing functions, that were implemented in order to re-arrange data into a form, that could be suitable for feeding the intelligent control module. That part of the system is the one that can be seamlessly adapted to different types of domains, even other than subways. Also, in literature the importance of the role of WSNs for monitoring the dynamics of an indoor environment to implement anticipatory optimal control policies was discussed [2]. In Section 2 of this paper, we will report the features of the WSN installed, including reasons, design constraints and lessons learnt. In section 3 we will look into the technical details of the post-processing functions, that were implemented to extract useful information from the raw data supplied by the WSN.

2 Wireless Sensor Network for Environmental Monitoring

The main objective of the SEAM4US project is energy savings in underground transportation systems through optimized control of the station subsystems, such as ventilation and illumination. To this aim, modelling of the environment is the first essential step.

In order to fulfil these requirements, a Wireless Sensor Network (WSN) was deployed in the historic metro station of Passeig de Gracia in Barcelona, consisting of 38 sensor nodes and 4 sensor gateways

that have been installed in several areas. In this section, we explain in detail the requirements of the project as well as the limitations and challenges encountered during deployment and data collection, and we discuss the main criteria of the specific choices. Finally, we highlight the main lessons learnt during the installation and testing, and provide some insights about data delivery reliability and energy efficiency of the system.

2.1 Requirements, constraints and challenges

Efficient modelling of the system entails accurate environmental sensing and reliable data delivery, so as to acquire a complete representation of the operational context. On one hand, the system configuration needs to be flexible, so that the initial setting can be changed over time to respond to new requests or changes in the environment. On the other hand, the location of sensor nodes was fixed and could not be easily modified after the installation.

The sensor nodes placement is driven by a combination of several different requirements, conditions and limitations of the environment itself. The metro station Passeig de Gracia is one of the most crowded in the city, connecting three important railway lines and having on average more than fifty trains per hour. This is a harsh environment for sensor placement, operation and communication, as many station areas are located far from each other, many obstacles can severely affect the signal propagation, and it is a highly dynamic scenario due to the significant number of passengers and trains crossing the station every day.

The location and distance among the sensor nodes must guarantee reliable connectivity to the central SEAM4US server for all sensing nodes. The station area is rambling, thus direct links to the gateway are not always possible. Indeed, connecting all nodes directly to the gateway was neither feasible nor efficient, but the network architecture was done in such a way to provide multi-hop paths from all nodes to the gateway. The actual location of a sensor is also limited by the station structure, including stairs and corridors, and by objects such as panels and pipes along the walls, but it has also to guarantee hard reachability to limit potential damage and vandalism.

Maintenance is an expensive task in this kind of environment due to many reasons, such as the limited time in which it can be done - we were allowed to work only for few hours during the night -, the hard-to-reach location where many sensors are installed, and it can be demanding in terms of time and cost to reach the place if it is not in the vicinity, as in our case (i.e. from Oulu to Barcelona). This implies the need for a system with very low power consumption to limit the need of battery replacement, as well as the need to the keep the number

of costly tasks limited (e.g. calibration).

Finally, an essential requirement of such a system is that it must be robust against unexpected events, such as power outage or node/link failures, which are part of the environment and cannot be completely avoided. The system must be able to automatically recover from this kind of situation, without necessarily requiring manual intervention.

The requirements of the monitoring application were defined in terms of the areas to be monitored, the environmental aspects to be measured and the sensor activity. Hence, the amount of sensor nodes to be installed, the sub-areas and the more precise location to be monitored were decided based on these requirements together with the limitations discussed above. Concerning the measurement task, each sensor node has to sense the environment every minute and send the measurement to the gateway server every 10 minutes.

2.2 Design choices and criteria

Several sensor nodes were installed inside the metro station, each of them sensing a specific set of environmental aspects under investigation. The sensors are all implemented on the processing and communication board by Redwire LLC called Econotag, with an additional 32 KHz oscillator and one of the 4 sensor boards specifically designed to fulfill the requirements of the project. Table 1 lists all of them, reporting the specific environmental aspects measured through every board. In addition, Figure 1 illustrates how the WSN is installed within the station, also showing that the network is divided in 4 sub-networks from the communication point of view (SN2,SN3,SN4,SN5), whereas SN1 includes only the weather station.

One of the most important design choices was to deploy a wireless network, as the need for wiring all the nodes can easily limit the installation options. For similar reasons, most of the sensor nodes are battery powered, whereas all the sensor gateways have power supply, in order to guarantee continuous operation. The position of sensors was decided according to the specific requirements for modelling and controlling the system. Due to the limitation mentioned above, it is often necessary to choose a trade-off between requisites from monitoring, wireless communication and building structure.

This is the case of all but the types of nodes we have installed: air temperature and parameters of indoor air quality should be estimated as the average value out of a set of measurements spread throughout any room. Similarly, air speed through corridors or entrances should be measured in several locations scattered on a cross section. But, the main issue consisted in keeping

passageways and corridors free from obstacles; in other words, no interference between users and WSN was allowed. So, sensors were placed as close as possible to desired positions, then a calibration process was applied to estimate at what extent measurements were affected by their sub-optimal locations and, when feasible, correction factors were applied.
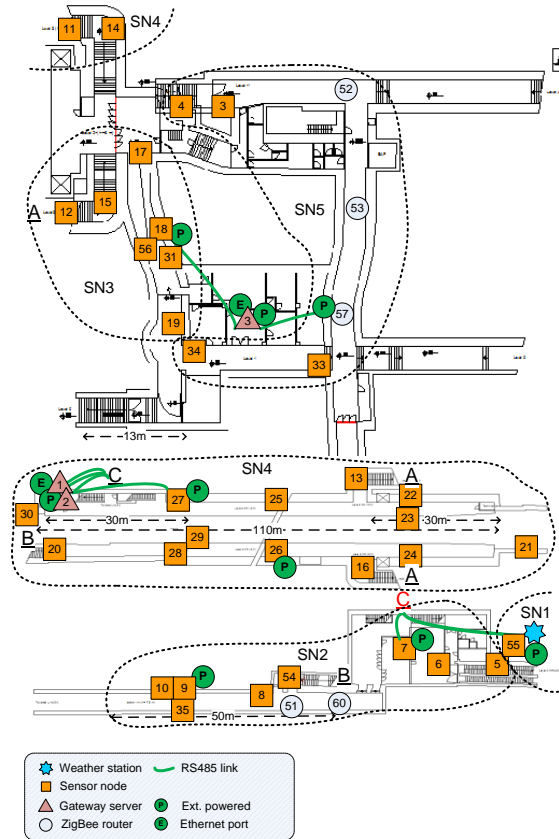

Figure 1. Sensor node positions.

Routing plays a key role to ensure correct data delivery. To allow multi-hop communication and adapt to the variable condition, we implemented a dynamic routing protocol to achieve flexibility and quicker set up. Indeed, the protocol periodically exchange a very restricted amount of information, taking advantage of other control packets, so that routing information are update frequently, but the amount of additional control traffic is very low. The actual ad-hoc routing procedure, involving more control packet to be exchanged, is used only in case of missing information. The routing algorithm takes both link quality and hop-count into account, in order to better capture the quality of each available path.

To reduce the risk of damage and vandalism, sensor nodes were protected by a plastic box and they were installed on the wall or the ceiling in positions

difficult to reach. In fact, only 2 sensors out of 42 were damaged or lost during the testing period.

Each sensor acquires its settings from the gateway after reboots and error conditions, and it stores some previous measurements. This approach significantly reduced the negative effect of node failure, worsening of the signal propagation and unexpected events that could not be known or prevented in advance, such as events in the city that significantly change the activity and occupancy of the metro station. As random access and reconfiguration was needed, the battery operated sensors with microcontroller were preferred instead of those with energy harvesting capability. Also, the battery operated nodes are usually cheaper. Concerning power saving, we implemented an energy efficient MAC protocol that combines R-MAC [3] and ContikiMAC [4], leading to a cross-layer mechanism able to allow nodes to stay in sleep mode most of the time, according to the application's data sampling and delay requirements [5]. This way, we are able to achieve battery replacement periods of many years, as shown from the estimation in Figure 2, which was satisfactory for this use case.

Motivated by the calibration-related issues, and having the possibility to remotely re-configure the nodes, some auto-calibration features were implemented, reducing the need of actual calibration.

Table 1 Sensor boards

Type	Probes	Sensor IDs
Sensor Board 1	-Air pressure -Air temperature -Surface temperature -High-speed anemometer	1, 3, 4, 5, 6, 7, 8, 10, 11, 12, 13, 14, 15, 16, 17, 18, 20, 21, 22, 23, 24, 25, 27, 28, 29, 30, 31, 32, 33, 34, 57
Sensor Board 2	-Air pressure -Relative humidity -CO_2 -PM10	26, 35
Sensor Board 3	-Air temperature -Surface temperature -Low-speed anemometer -Differential pressure	9, 56
Weather Station	-Solar radiation -CO_2 -PM_{10}	55

In fact, after the deployment and collection of environmental data, the application was only considering relative and not absolute values, which was not decided at the beginning. For this reason, the

calibration was not necessary anymore, although the initial cost of the devices could not be changed at that point.
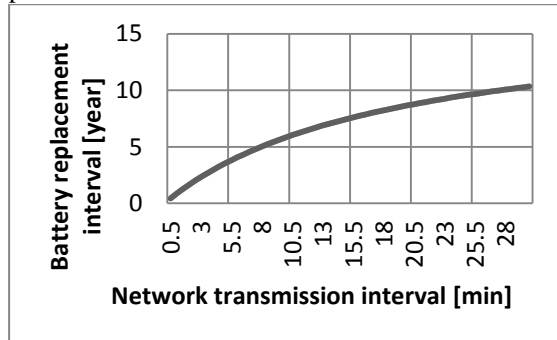

Figure 2. Battery replacement period for various transmission intervals.

Data reliability was strengthened by implementing a mechanism that periodically verifies the data received at the gateway server and requests data re-transmission in case of missing values. In practice, real-time monitoring is more strict in terms of delay requirements, hence the mechanism parameters must be tuned according to the specific requirements. During the modelling and testing time, the design of the monitoring network turned out to be redundant both in terms of measurements collected and in terms of available adjacent nodes for routing, due to some changes in terms of requirements. Clearly, in this kind of harsh environment, redundancy is often needed or desired, as it contributes to increase the reliability of the system.

2.3   Lessons learnt

The system can be configured remotely, thus allowing adaptation to variable requirements and conditions, as well as checking for issues and acquiring data for analysis. This approach limits the need to go physically into the station, which is especially convenient in case of long distance, and during the testing phase - where many more accesses to the system may be needed compared to when the system is more stable.

The remote access has, however, some limitations, as some issues cannot be faced remotely, and people solving issues are not always aware of the actual operational conditions and causes of the problems. For example, some corridors can be closed temporarily for maintenance and renovation, as it happened in our case, which may cause significant changes in measurements and network performance. If people performing remote analysis do not know about the closure, they may misunderstand the reason of the change and apply unnecessary and potentially inconvenient fixes, such as extra calibration. Hence, it is important to acquire as

much up-to-date information as possible on any aspect that can impact on network performance and operation. Indeed, even sensor placement could have been different in our case if we had the possibility to know some of the renovation plan in advance, as some of the installed sensors became practically not accessible for maintenance or usable for communication, due to additional structures, such as walls.

Generally speaking, if the environment is harsh and there are several constraints, then having the most complete view of the environment is important for designing, deploying, testing and evaluating, and in turn to make the system robust and reliable. Also, being sure to be informed about all the planned events and activities that can affect the station operation and conditions, limits the likelihood of misinterpreting changes in the system and taking inappropriate actions.

Finally, choosing between short range high bandwidth and longer range lower bandwidth communication is another crucial aspect. In fact, in our deployment we preferred the former solution to allow remote update and configuration, but it caused some issues in the installation in terms of number of necessary nodes and installation location to ensure monitoring coverage and communication. Hence, the choice depends on many factors that vary from scenario to scenario, and must be all considered in advance.

2.4   System performance

The requirement in terms of data delivery can be summarized by specifying the maximum allowed packet loss as 20%. In fact, the system was able to satisfy the requirement as the average packet delivery ratio over the entire network during the evaluation period was 13%. An interesting finding is that in this kind of environment, sub-networks can show significant differences in terms of performance compared to other more homogeneous scenarios. For a quick look at this aspect, in Table 2 we reported the values of some performance indicators observed during a period of one week, both the average value over the entire network and the average for each sub-network: the packet loss (PL), the number of hops to the gateway (NH) and the number of available routing paths to the gateway (NP). The total average is not the average of the values shown below, since each sub-network has different number of nodes. The sub-network SN4 is the one that cover the tunnel where on average one train every minute passes, implying that it is located in a very dynamic environment mainly due to passengers and trains crossing. As you can see from Table 2, SN4 is the sub-network with the lowest packet loss and the higher number of available paths. Indeed, we could

observe that the number and position of sensor nodes in SN4 was sufficient to ensure many multi-hop alternative paths for each node, despite the challenging condition. On the other hand, SN5 has the highest packet loss, mainly because each node has very limited alternative paths to reach the gateway, and renovation areas surround or partially cover this area, limiting communication and worsening channel condition. Hence, we can say that in harsh environments it is important that every node has some alternative paths to reach the central server, as this redundancy contributes to reduce the packet loss..

Table 2. Packet loss ratio of the WSN.

average	PL	NH	NP
TOT	13%	2.04	17.34
SN2	7%	2.19	16.8
SN3	24%	2.3	4.25
SN4	5%	1.9	31
SN5	35%	1.77	1.6

3   The monitoring sub-system

The main task of the monitoring sub-system is to act as an interface between the model used to drive the control logics and the data gathered by means of the WSN described in section 2. Indeed, the control model accepts as inputs synchronized clean data, complete records at regular time intervals. However, this is not the case of raw data sent by the WSN. For that reason, the monitoring sub-system was made up of a set of units developed to recover a data flow from the WSN and convert them into a suitable form for feeding the control model's computations. As a consequence, three main steps are accomplished by this component: 1) filtering, 2) re-sampling and 3) post-processing. Step no. 1 aims to reduce noise of raw data and aliasing; the second step performs time alignment; finally, the last step may include a number of functions, among which we cite unit conversion, calibration and estimation of indirect measurements.

3.1   Architecture of the monitoring sub-system

The raw data are redirected from the WSN to the monitoring sub-system via proxy devices. The raw measures listed in Table 1 are processed: air temperature, CO_2 concentration, PM_{10} number of particles, relative humidity, wind speed, wind direction, air speed. All these variables are then filtered and resampled, while some of them are post-processed, too. The whole picture is shown in Figure 3.

Focusing on the estimation of air changes per hour, the WSN acquires one value about air speed and air temperature through some critical cross sections of the PdG station. All the raw measures are asynchronously acquired. Those data are then sent to the monitoring sub-system via the corresponding device proxies. They are filtered in order to reduce noise and alias and re-sampled, i.e. aligned in time according to a preset time scale. Then, some post-processing functions (that will be described later on) are implemented, so as to work out air flow rates from air speed measurements. Then, the estimated air flow rates are combined and summed up, according to the combination of pathways through which air in the station is flowing. Such a combination gives back the air change rate of the whole station. Raw data are sampled with an approximate time step $T_s \cong 60s$, varying according with the quality of the wireless communication. They are filtered with a cutoff frequency $F_{cut} = 1/T_f$ (i.e. frequency at -3dB of attenuation), and then resampled every T_r seconds.

Filtering is used to smooth data but it introduces delay in data that, when too long, could make the information useless for control purposes. Delay introduced by the filter depends on filter order, type and cutoff frequency (i.e. frequency at -3dB of attenuation) with respect to sampling frequency $F_s = 1/T_s$. IIR filter was selected and used as best compromise between complexity, selectivity and phase shift:

$$y_n = (1 - a)x_n - ay_{n-1} \tag{1}$$
$$a = e^{-2\pi F_{cut}/F_s} \tag{2}$$

The choice of T_r depends on a couple of factors: on one side the disturbances affecting raw measures, because the stronger the disturbances are, the lower the filter cutoff frequency is, the longer T_r is, the higher the filter delay is. On the other hand, the controlled dynamics requires that the faster the dynamics to be controlled is, the shorter T_r must be. Therefore, in order to have a short reaction time for control action, resampling interval should be kept as small as possible. From frequency domain and time-domain residual analysis of raw data, the best filtering period was found to be $T_f = 1/F_{cut} = 1200$. Therefore, by considering negligible spectral components above cutoff frequency of the filter, according to the sampling theorem, resampling rate must be at least twice the maximum frequency of the signal to be sampled $\frac{1}{T_r} \geq 2F_{cut} = 2\frac{1}{T_f}$.

For keeping small T_r, in our case the limit value was used $T_r = T_f/2 = 600s$. From now on, post processing functions will be applied to all filtered and resampled values.

3.2 Post-processing functions

In this section, we will look into three types of post processing functions, that were implemented in the Sem4us system, and that were used to estimate the following variables, that are forwarded to the control sub-system: air change rates; air temperature values; dust (PM_{10}) concentration.

3.2.1 Air change rates

Air change rates in the platform (i.e. the most crowded room in the station) were derived straight from a sum of air flow rates through corridors. In fact, this station is made up of several corridors leading to the platform.

Hence, if air flow rates through them are estimated in real-time, the total amount of outdoor air provided in the platform at each time step can be estimated. To this purpose, a vital input is the measure of air speed flowing through corridors, that was carried out by means of the "high speed anemometer" reported in Table 1. Such a device is sheltered by a pipe on its sides and by a net at the pipe's ends, in order to prevent debris from soiling its rotating impeller and vane. Both sheltering and the need for locating anemometers close to one of the room's top corners may compromise the quality of the measure. For that reason, a comparison between the measurements from this device and those ones from a hand-held instrument was used for calibration. The calibrated measurements of air speed were then multiplied by the cross section, so as to work out air flow rates. The validity of this procedure was already demonstrated by the authors in a previous research paper [8]. More specifically, numerical simulations supported by experimental evidence

showed that obstacles that may be found in corridors (e.g. people) affect only locally air speed field in any cross section of corridors, and do not change the overall balance estimated in the case of unobstructed corridor's cross section. This confirms the validity of the straight multiplication between cross section's area and average air speed. Another finding was that, on the contrary, trains in tunnels affect the amount of air flow rates across tunnels. As a consequence, air flow rates in tunnels were reduced by a factor, that was computed as a result of an overall air flow balance in the station.

The calibration curve that was used to adjust measurements of high speed anemometer includes an y-offset (q) and a scale factor (m):

$$Q = m \cdot Q' + q \tag{3}$$

The two coefficients were estimated from a set of on ground measurements performed in the station. The dataset was then split into the first 75%, that was used for estimating the coefficients q and m, and the second 25%, that was used for validation purposes. Technically, the estimation was based on an OLS (Ordinary Least Square) algorithm [6]. Six calibration curves were worked out for as many sensors. Each curve was based on two sets of measurements taken for about 15 min at two different times of the day.

In Figure **4** an example of the inputs and outcomes from this calibration process is provided. Figure **4**-a compares the plot of the data logged by the hand-held instrument (i.e. benchmark) and the data plotted by the installed Seam4us sensor, where the benchmark presents peaks higher than the Seam4us sensor, and its average value is slightly higher than the other series. Those plots are the result of filtering and resampling, as reported in sub-section 3.1. Then, the y-offset (0.1510 m/s) and scale factor (1.2719) of the calibration curve were estimated by means of OLS analysis, like in eq.
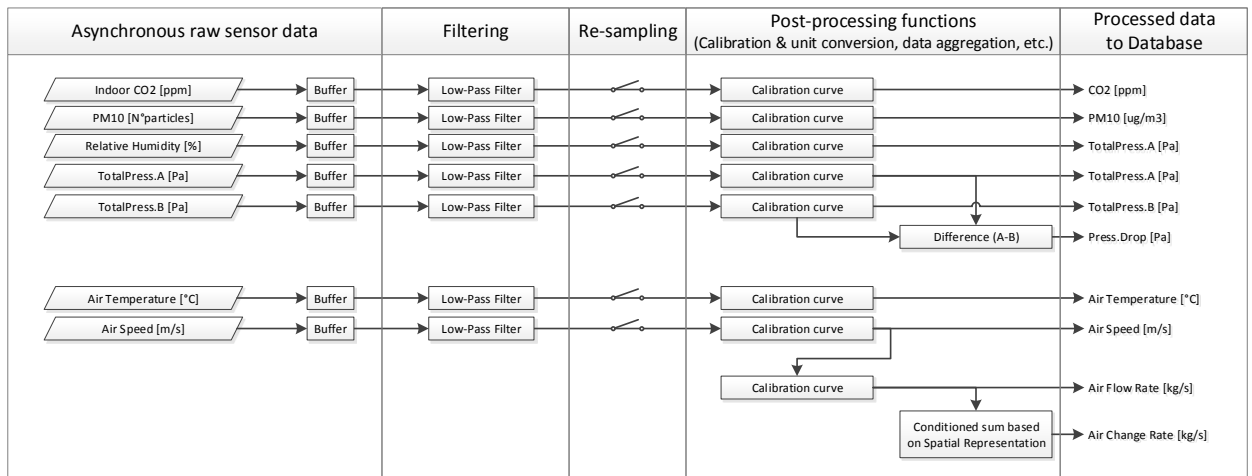

Figure 3. The most critical monitoring functions for the main parameters of the WSN.

(3). Similarly, the calibration curves for all the other corridors were worked out. In the case of node no. 18, Figure **4**-b shows that the calibration brought the two curves to almost superimpose. At this juncture, air flow rates through corridors are known and they are ready to be combined one another in order to estimate outdoor air supplied to the platform (PL3), that is air change per hour from outdoor air (ACO):

$$ACO_{PL3} = Q_{as} + Q_{CNl} + (Q_{CNe} - Q_{SLb})^+ \qquad (4)$$

where Q_{as} is the air supplied by the mechanical ventilation system; Q_{CNl} is air flow rate entering through corridor CNl, and the last two terms computes the difference between air flow rate flowing through corridor CNe and another corridor called SLb. The difference was due to the evidence that only the air flow coming from CNe, but that was not directed towards SLb, entered the platform PL3. The plus apex indicates that this contribution was taken into account just in case the balance is positive. Although no contribution to the platform's daily ventilation came from the two Pdg's tunnels, because they always worked in extraction mode, the reduction determined on air flow rates due to the presence of trains was estimated just for the purpose of general knowledge. The overall air flow balance in the station around the platform can be written as:

$$-Q_{as} = Q_{CNl} + Q_{CNq} + 2 * Q_{CNop} + \alpha \cdot Q_{tun} \qquad (5)$$

where, Q_{as} is the air flow rate of the fans injecting air in PdG, Q_{tun} is the air flow rate of the fans extracting air from tunnels and CNl, CNq and CNop are corridors, where the direction of air flow may change over time. The overall air flow balance brought to determine the coefficient $\alpha = 0.7$, that is the reduction due to the presence of trains in tunnels.
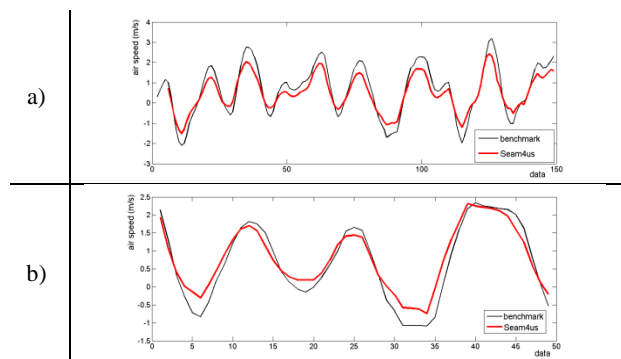

Figure 4. First 75% raw data at node no. 18 (corridor CNl) and transformed curves compared with the remaining 25% of the dataset.

3.2.2 Air temperature

Similarly to what described in sub-section 3.2.1, air temperature plots provided by the Seam4us' WSN were compared with those ones measured by accurate hand-held instruments. We checked two types of deviation: an y-offset of the respective average values of the two plots; peaks of the Seam4us networks were lower than the peaks of the hand-held instrument. The latter was probably due to the packaging inside which the Seam4us sensors were sheltered. But it was deemed as not relevant, because just average temperatures over time steps of one hour were needed by the intelligent control module, whereas peaks were due just to trains passing by, whose consequences lasted for a few minutes. The former was corrected by comparing the two average measures from the two plots and applying an y-offset factor to every Seam4us sensor, in order to match the measurements collected by means of the benchmark. So, one y-offset for each Seam4us temperature sensor was estimated.

3.2.3 Dust concentration

The raw measurements provided by the PM_{10} sensors installed indoors were relative to the number of particles counted within 0.283 l of air volume (pcs/0.283 l). The purpose of the post-processing function was twofold: firstly, to extend particles' count over the whole spectrum, due to the fact the sensor was able to sense only particles sized more than 0.5 μm; secondly, PM10 concentration should be measured in standard unit of measure, i.e. μg/m³. In order to pursue that, a post-processing function made of six steps was set up. Given that raw data (*rawPM*) were measured as pcs/0.283 l, the first step turned it into *n* measures in pcs/m³, through the factor $k = 3534$ l/m3, hence $n = k*IndPM$. The second step assessed the ratio of particles out of their total number, that was not considered in the raw measures (because limited above 0.5 μm). So an on-site survey through a hand-held instrument (i.e. "Fluke particle counter") was done, and the distribution in Table **3** was had. As a result, if the sum of particles measured by the WSN between 0.5 and 10 μm is 100%, that number must be increased by 79.3% to include even those particles between 0.3-0.5 μm.

Table 3. Distribution of particle size in PdG.

Diameters [μm]		Ratio D^j [%]
Range	Central value [d_s^j]	
0.3 – 0.5	0.4	79.3
0.5 – 1.0	0.75	62.2
1.0 – 2.0	1.5	19.1
2.0 – 5.0	3.5	17.7
5.0 – 10.0	7.5	0.88
> 10.0	12.5	0.13

Given the distribution of particles in Table **3**, in the third step the number of particles per size was rewritten in the form: $n^j = n * D^j$, where n^j is the number of particles whose diameter's central value is equal to d_s^j, n is the raw measure of particles and D^j is the ratio. Steps 4 to 6 were determined according to literature, and used to convert the number of particles in concentration. In particular, step no. 4 computed the volume occupied by n^j particles [9]:

$$vol^j = \frac{\pi}{6} \cdot \left(d_s^j\right)^3 \cdot n \qquad (6)$$

As a fifth step, the concentration m^j [μg/m^3] will be computed as [10]:

$$m^j = C_F \cdot \rho_{eff}^j \cdot vol^j \qquad (7)$$

where the coefficient $C_F = 1$ in our case and an overall value of ρ_{eff} was assessed experimentally according to the relationships [11]:

$$\rho_{eff} = \frac{PM_{10}}{\Sigma_{j=1}^5 vol^j \cdot F_{PM10}^j} \qquad (8)$$

The coefficients F are provided by literature [11], while PM_{10} was measured in the station, at the same time when the counting in Table **3** was done. It came out that $PM_{10} = 320$ μg/m^3, all the other values are known, hence $\rho_{eff} = 3.15 \cdot 10^{12}$ μg/m^3.

By combining all the steps described above, the conversion of the kind depicted on Figure **5** were performed automatically by the Seam4us system, and in real-time during monitoring.
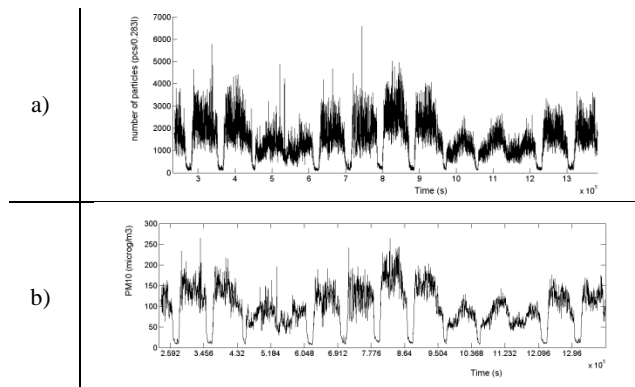

Figure 5. Example of post processing for PM_{10} applied to room SLb in the PdG station.

4   Conclusion

In this paper, the wireless sensor network and the post-processing functions implemented in the PdG (line no. 3) subway station in Barcelona were described. The main purpose of this system was to sense in real-time the environment and to redirect processed data to the intelligent control unit, that was in charge of controlling the station's subsystems according to actual users' behaviour and boundary conditions.

The main issues leading to a correct installation of the WSN and the computational protocols implemented for post-processing the main environmental variables were detailed. The results from post-processing showed that, thanks to this approach, it was possible to assess in real-time the dynamics of those environmental variables that are critical to describe the behaviour of the station and to drive the intelligent control system of PdG.

References

[1] SEAM4US – Sustainable Energy mAnageMent for Underground Stations, 2011. Seventh Framework Programme, Grant Agreement No: 285408.

[2] Mahdavi, A., Orehounig, K., Pröglhöf, C., 2009. *A simulation-supported control scheme for natural ventilation in buildings*. In: Proceedings of the 11th IBPSA Conference, Glasgow, Scotland.

[3] Koskela P., Valta M., Frantti T., *Energy efficient MAC for wireless sensor networks*, Sensors and Transducers Journal, vol. 121, no.10, pp.133 – 143, Oct.2010

[4] Dunkels, *The ContikiMAC Radio Duty Cycling Protocol*, SICS, Tech.Rep. T2011:13, Dec. 2011.

[5] Hiltunen J., Valta M., Ylisaukko-oja A. and Nurchis M., *Design, Implementation and Experimental Results of a Wireless Sensor Network for Underground Metro Station*, IJCSCN, vol. 4, no. 3, pp. 58 – 66, July 2014

[6] Wonnacott T. H. Wonnacott R. J. *Introductory statistics*, John Wiley and sons, 5th ed., ISBN: 0-471-615-18-8

[7] Ling K. V., Maciejowski J. M., Guo J. Siva E., *Channel-Hopping Model Predictive Control*, IFAC, 2011.

[8] Di Perna C., Carbonari A., Ansuini R., Casals M., *Empirical approach for real-time estimation of air flow rates in a subway station*, Tunnelling and Underground Space Technology, Volume 42, May 2014, Pages 25-39.

[9] William C. Hinds (1999) *Aerosol technology*, John Wiley and Sons, Inc.

[10] Paul A. Baron, Klaus Willwkw (2011), *Aerosol measurements*, Wiley Interscience ed.

[11] De Carlo P. F, Slowik J. G., Wornop D. R., Jimenez J. L., *Particle morphology and density characterization by combined mobility and aerodynamic diameter measurements. Part 1: theory,* Aerosol Science and Technology, 2004.